Available online at www.sciencedirect.com

ScienceDirect

journal homepage: www.elsevier.com/locate/issn/15375110

Research Paper

Simulation and prediction of radio frequency heating in dry soybeans

Zhi Huang [a], Hankun Zhu [a], Rongjun Yan [a], Shaojin Wang [a,b,*]

[a] College of Mechanical and Electronic Engineering, Northwest A&F University, Yangling, Shaanxi 712100, China
[b] Department of Biological Systems Engineering, Washington State University, Pullman, WA 99164-6120, USA

ARTICLE INFO

Article history:
Received 8 November 2013
Received in revised form
17 March 2014
Accepted 23 September 2014
Published online

Keywords:
Computer simulation
Dielectric heating
Disinfestation
Heating uniformity
RF

Radio frequency (RF) heating is considered as a potential postharvest technology for disinfesting legumes. However, the non-uniformity in RF heating is still a major problem in developing effective RF heat treatments for pest control and other applications. A computer simulation model was developed with a finite element-based commercial software, COMSOL, to analyse the temperature distributions. Dry soybeans packed in a rectangular plastic container were used to determine the heating uniformity and validate the simulation model using a 27.12 MHz, 6 kW RF system. Both simulated and experimental results showed similar heating patterns in RF treated soybeans, in which corners and edges were more heated and the temperature values were higher in the lower part of the container. The simulation results demonstrated that the RF heating uniformity could be improved using a similar dielectric material around the samples, a smaller top plate area (similar to the sample size), and placing the samples in the middle of the two plate electrodes. The simulation model developed in this study could be applied to improve the RF heating uniformity and to optimise the treatment parameters.

1. Introduction

Soybean (*Glycine max*) is a leading oilseed crop produced and consumed worldwide because of its broad uses for human and animal food, industrial and medical applications (Wilcox, 2004). But a major problem in storage, production and marketing of soybeans is infestation by insect pests (USADPLC, 2007). These pests degrade the soybean quality by direct damage through feeding and webbing the production, and indirect damage through induction of diseases, which may pose a critical threat to consumer health. To meet phytosanitary and quarantine regulations for international trade, there is an urgent need in developing non-chemical postharvest pest control methods for dry soybeans.

Radio frequency (RF) energy is an electromagnetic wave with a frequency of 1–300 MHz, which provides rapid and volumetric heating, and has been studied as a non-chemical alternative for postharvest insect control in dry products (Halverson, Burkholder, Bigelow, Nordheim, & Misenheimer, 1996; Nelson, 1973; Tang, Ikediala, Wang, Hansen, & Cavalieri, 2000), such as alfalfa seed (Yang, Zhao, & Wells,

* *Corresponding author*. College of Mechanical and Electronic Engineering, Northwest A&F University, Yangling, Shaanxi 712100, China. Tel.: +86 2987092391; fax: +86 2987091737.
E-mail addresses: shaojinwang@nwsuaf.edu.cn, shaojin_wang@wsu.edu (S. Wang).
http://dx.doi.org/10.1016/j.biosystemseng.2014.09.014
1537-5110/

Notation

A	top plate area (mm^2)
c_p	heat capacity ($J\ kg^{-1}\ K^{-1}$)
d	distance (m)
E	electric field intensity ($V\ m^{-1}$).
f	frequency (Hz)
k	thermal conductivity ($W\ m^{-1}\ K^{-1}$)
m	moisture content (w.b.)
Q	density of power generated by electric field distribution ($W\ m^{-3}$)
t	time (s)
T	sample temperature (K)
V	electric potential (V)
V_{vol}	sample volume (m^3)
z	vertical co-ordinates or vertical position (m)
α	thermal diffusivity ($m^2\ s^{-1}$)
ε_0	free space permittivity ($F\ m^{-1}$)
ε'	dielectric constant (dimensionless)
ε''	dielectric loss factor (dimensionless)
∇	gradient operator
ρ	density ($kg\ m^{-3}$)
σ	electric conductivity ($S\ m^{-1}$)

Subscripts

mat	material
av	average
vol	volume

2003), grain (Nelson, 1996), legume (Jiao, Tang, Johnson, Tiwari, & Wang, 2011; Wang, Tiwari, Jiao, Johnson, & Tang, 2010), lentil (Jiao, Johnson, Tang, & Wang, 2012), rice (Lagunas-Solar et al., 2007; Zhao, Qiu, Xiong, & Cheng, 2007), walnut (Mitcham et al., 2004; Wang et al., 2001; Wang, Monzon, Johnson, Mitcham, & Tang, 2007a, b; Wang et al., 2006), and wheat (Halverson et al., 1996). The relatively long wavelength of RF usually results in deep penetration depth and predictable temperature profiles in foods, but the non-uniform heating is still a problem for RF heating technology to be applicable in the food industry (Tang et al., 2000; Wang et al., 2007a). The different temperature distribution among and within products may cause quality loss or insect survival due to overheating in corners and edges, and under-heating in centre parts, especially in foods with intermediate and high water contents (Fu, 2004). It is essential to understand the complex mechanism of RF heating and improve the heating uniformity in RF treated products so as to ensure complete insect mortality and maintain product quality throughout the whole product volume.

Computer simulation and mathematical modelling serve as a valuable tool for rapid analysis of RF heating process without the necessity of extensive time consumed in experiments. Computer simulation has also been conducted to study the RF heating uniformity in various food materials, such as alfalfa and radish seeds (Yang et al., 2003), 1% carboxy methyl cellulose solution (Chan, Tang, & Younce, 2004), cylindrical meat batters (Marra, Lyng, Romano, & McKenna, 2007), meat (Romano & Marra, 2008), fresh fruits (Birla, Wang, & Tang, 2008; Birla, Wang, Tang, & Tiwari, 2008), mashed potato (Wang, Olsen, Tang, & Tang, 2008), wheat flour (Tiwari, Wang, Tang, & Birla, 2011a), and raisins (Alfaifi et al., 2014). Neophytou and Metaxas (1996, 1998, 1999) attempted to model the electrical field for industrial-scale RF heating systems by solving the coupled Laplace and wave equations. The well-developed computer simulation model makes it possible to obtain accurate results from various agricultural products. Different criteria and indexes have been used to study, evaluate, and compare the RF power and temperature uniformity in food samples, such as the normalised RF power density (Neophytou & Metaxas, 1998), the heating uniformity index (Wang, Yue, Tang, & Chen, 2005), the RF power uniformity index (Tiwari, Wang, Tang, & Birla, 2011b), and the temperature uniformity index (Alfaifi et al., 2014). Since the sample temperatures are the main targets in RF heating for disinfestations or pasteurization and quality evaluations, the simulated temperatures in dry food samples are accessed and compared under different conditions using the simulated temperature uniformity index (STUI) in this study.

There are few reports on the computer simulation and prediction about effects of related parameters on the RF heating uniformity in dry soybeans for thermal disinfestations. Therefore, it is necessary to systematically study the RF heating characteristics and evaluate treatment parameters to improve the RF heating uniformity in dry soybeans based on the validated computer simulation model. Specific objectives were to (1) develop a computer simulation model for dry soybeans when subjected to a 6 kW, 27.12 MHz RF system using commercial finite element software COMSOL, (2) validate the computer simulation model by comparing with the transient experimental temperature profiles of dry soybeans at three different layers after 6 min RF heating, and (3) apply the validated computer simulation model to predict the effects of sample moisture content, top electrode area, sample vertical position, and special dielectric container materials around samples on the behaviour of RF heating uniformity in dry soybeans.

2. Materials and methods

2.1. Sample preparation

Seeds of soybean were purchased from a local grocery store in Yangling, Shaanxi, China and stored at the constant temperature (25 °C) of a thermostatic and humidity controlled chamber (BSC-150, Shanghai BoXun Industrial & Commerce Co., LTD., Shanghai, China) prior to RF experiments. The composition of soybean was reported on the label as: 11.2 g $(100\ g)^{-1}$ fat, 35.1 g $(100\ g)^{-1}$ protein, 5.0 g $(100\ g)^{-1}$ ash, 41.1 g $(100\ g)^{-1}$ sodium, and 41.1 g $(100\ g)^{-1}$ carbohydrate (Guo, Wang, Tiwari, Johnson, & Tang, 2010). The initial moisture content of dry soybean was $5.13 \pm 0.11\%$ on wet basis. The bulk density of dry soybean at room temperature was measured by a basic volume method using a $30 \times 22 \times 6\ cm^3$ plastic rectangular container and obtained to be $748 \pm 4\ kg\ m^{-3}$ over three replicates.

2.2. Computer simulation

2.2.1. Physical model

A 6 kW, 27.12 MHz parallel plate RF heating system with a free-running oscillator (COMBI 6-S, Strayfield International Limited, Wokingham, UK) was used in this study for dry soybeans heating experiments (Fig. 1). The RF system included a generator and an applicator, which consisted of two parallel metal plate electrodes inside a large rectangular metallic enclosure. The space between the two electrodes formed a cavity that filled with electromagnetic field in operation. The top electrode position could be changed to adjust the electrode gap and the bottom electrode was fixed with the metallic enclosure. The food material (dry soybeans) in a container was placed on the bottom (ground) electrode. The dielectric material in the cavity was heated up due to the energy conversion from electromagnetic energy to heat.

2.2.2. Governing equations

2.2.2.1. Electric current. The electric field intensity in the electromagnetic field was solved by the Maxwell's electromagnetic field equations. Since the wavelength (11 m) of electromagnetic wave in the 27.12 MHz RF system is usually much larger than the RF cavity size (1.29 × 1.09 × 0.74 m^3),

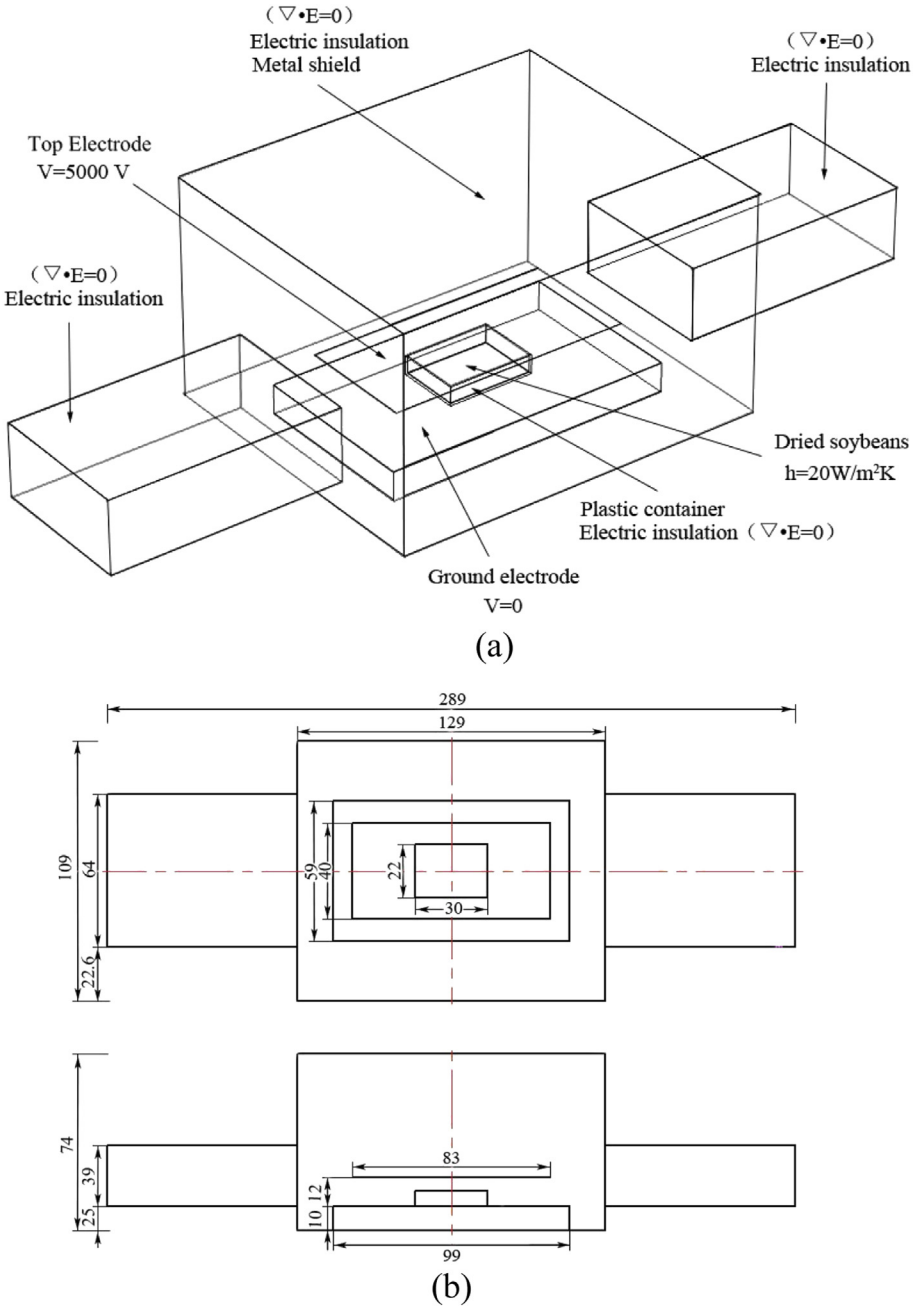

Fig. 1 – 3-D Scheme (a) and dimensions (b) of the 6 kW, 27.12 MHz RF system and food load (dry soybeans) considered in simulation (all dimensions are in cm).

Maxwell's equations can be simplified to Laplace equations with a quasi static assumption (Birla, Wang, & Tang, 2008; Choi & Konrad, 1991):

$$-\nabla\cdot((\sigma + j2\pi f\varepsilon_0\varepsilon')\nabla V) = 0 \quad (1)$$

where σ is the electric conductivity of food material (S m^{-1}), $j = (-1)^{0.5}$, f is the frequency (Hz), ε_0 is the permittivity of electromagnetic wave in free space (8.854 × 10^{-12} F m^{-1}), ε' is the dielectric constant of food material, and V is the electric potential between the two electrodes (V).

2.2.2.2. *Heat transfer*. The amount of power conversion from electromagnetic energy to thermal energy is related to the dielectric properties of treated materials. RF power conversion in the food is governed by (Metaxas, 1996):

$$Q = 2\pi f\varepsilon_0\varepsilon''|E|^2 \quad (2)$$

where Q is the power conversion to thermal energy in foods (W m^{-3}), ε'' is the loss factor of food material, and $E = -\nabla V$ is the electric field intensity in the food material (V m^{-1}).

By considering heat convection at the material's surface and the heat conduction within the food material, the heat transfer inside the food material is described by Fourier's equation:

$$\frac{\partial T}{\partial t} = \nabla\alpha\nabla T + \frac{Q}{\rho c_p} \quad (3)$$

where $\partial T/\partial t$ is the heating rate in food material (°C s^{-1}), α is the thermal diffusivity (m^2 s^{-1}), ρ and c_p are the density (kg m^{-3}) and heat capacity (J kg^{-1} K^{-1}), respectively.

2.2.3. *Initial and boundary conditions*

Figure. 1a and b show the geometrical and electrical boundary conditions of the 6 kW, 27.12 MHz RF system used in the simulation. The initial temperature was set as room temperature at 25 °C. Only the top surface of food sample was uncovered and exposed to air, and the sides and bottom were covered by the plastic rectangular container (Fig. 1). The convective heat transfer coefficient of the top surface was set as 20 W m^{-2} °K^{-1} for nature convection (Romano & Marra, 2008). The metal enclosure boundary of RF machine was considered as thermal insulation ($\nabla T = 0$). The top electrode was set as the electromagnetic source since it introduced the high frequency electromagnetic energy from the generator to the heating cavity and the bottom electrode was set as ground (V = 0 V). It was difficult to directly measure the high voltage during processing without disturbing the electric field (Marshall & Metaxas, 1998), so the voltage on the top electrode was assumed to be constant during the RF treatment and estimated by the following equation (Birla, Wang, & Tang, 2008):

$$V = \left(d_{air}\sqrt{(\varepsilon')^2 + (\varepsilon'')^2} + d_{mat}\right)\left(\sqrt{\frac{\rho c_p}{\pi f\varepsilon_0\varepsilon''}}\frac{dT}{dt}\right) \quad (4)$$

where d_{air} is the air gap between top electrode and food sample (m), and d_{mat} is the height of the food material (m).

The estimated voltages were 5000 V for simulation based on the heating rate in preliminary tests. All the metal shielding parts except for the top electrode were grounded, and considered as electrical insulation $\nabla\cdot E = 0$.

2.2.4. *Solving methodology*

A finite element method (FEM) based software COMSOL Multiphysics (V4.3a COMSOL Multiphysics, CnTech Co., LTD., Wuhan, China) was used to solve the coupled electromagnetic and heat transfer equations (Joule heating model). The software was run on a Dell workstation with two Dual Core 3.10 GHz Xeon processors, 8 GB RAM on a Windows 7 64 bit operating system. Figure 2 illustrates the steps taken in the simulation. Extremely fine tetrahedral mesh was generated in the food sample to guarantee the accuracy of temperature distribution results. Other parts of the system were meshed with normal size tetrahedral meshes. Mesh size was chosen based on the convergence study when the difference in the resulted temperatures between successive calculations was less than 0.1%. The initial and maximum time steps used in this study were set as 0.001 and 1 s, respectively. Each simulation task took around 18 min to finish.

2.2.5. *Model parameters*

The dielectric, thermal, and physical properties of the product and the surrounding materials are essential in modelling the RF heating process. The properties of dry soybeans, polypropylene and air at room temperature were listed in Table 1 for computer simulation. Dielectric properties of dry soybeans had a non-linear relationship with temperature and were measured before. Detail of the measurement system and procedure can be found elsewhere (Guo et al., 2010).

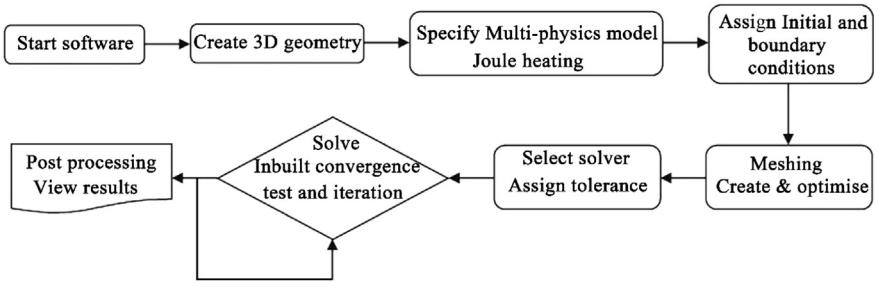

Fig. 2 – Flow chart of modelling steps using COMSOL Multiphysics (Alfaifi et al., 2014).

Table 1 – Electrical and thermo-physical properties of materials used for computer simulation.

Material properties	Dry soybeans	Aluminium[a]	Air[a]	Polypropylene[a]
Density ρ (kg m^{-3})	748[b]	2700	1.2	900
Thermal conductivity k (W m^{-1} K^{-1})	0.11[c]	160	0.025	0.26
Heat capacity c_p (J kg^{-1} K^{-1})	1737[d]	900	1200	1800
Dielectric constant	3.6[e]	1	1	2.0[f]
Loss factor	0.26[e]	0	0	0.0023[f]

Sources:
[a] COMSOL material library, V4.3a (2012).
[b] Measured only for model validation.
[c] Deshpande et al. (1996).
[d] Deshpande & Bal (1999).
[e] Guo et al. (2010).
[f] von Hippel (1995).

2.3. Model validation and prediction

2.3.1. Container material and dimension

A rectangular container (inner dimension was 300 × 220 × 60 mm^3) bottom and side walls were made of 3 mm thin polypropylene mesh (with mesh opening of 6.5 mm). To prevent soybeans falling out from the container, the internal surface of the plastic container was covered by a thin layer of gauze (thickness of 0.28 mm) with mesh opening of 1 mm.

2.3.2. Experimental procedure

The RF system was used in experiments to heat dry soybeans and then validate the computer simulation model. About 3 kg of dry soybeans were placed into the rectangular container positioned at the centre of the bottom plate between the two electrodes. The container filled with dry soybeans were horizontally divided into three layers and separated by two thin gauzes with mesh opening of 1 mm (Fig. 3). This was designed to make it easy for temperature mapping at multiple layers after RF heating. Prior to the RF treatment, the samples were equilibrated at room temperature (25 °C). A fibre optical sensor (HQ-FTS-D120, Xi'an HeQi Opo-Electronic Technology Co., LTD, Shaanxi, China) with an accuracy of ±1 °C was used and placed in the centre of the sample to monitor the temperature change versus time. The temperature-time history was recorded by the connected data logger (FTS-P104, Xi'an HeQi Opo-Electronic Technology Co., LTD, Shaanxi, China). When the central sample temperature reached 50 °C, the RF unit was turned off and the sample container was moved out for temperature mapping. The surface temperatures of soybeans in top, middle, and bottom layers in the container were immediately taken by an infrared camera (DM63-S, DaLi Science and Technology Co., LTD, Zhejiang, China) with an accuracy of ±2 °C. Details of the measurement procedure can be found in Wang et al. (2007a). The image analysis system (V1.0, DaLi Science and Technology Co., LTD, Zhejiang, China) was used to collect and analyse the surface temperature data points for each layer. A contour plot was used to present the isothermal curves of temperature distributions in three layers. The whole temperature measurement procedure was completed within 25 s. The experiments were replicated three times. The measured temperature profiles of soybeans in the container centre and three layers were compared with the simulated results.

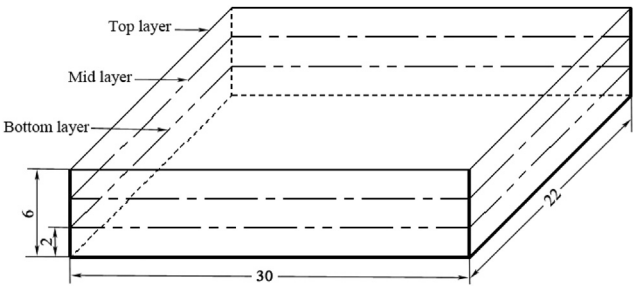

Fig. 3 – Rectangular plastic container split into three layers for temperature profile measurements (all dimensions are in cm).

2.4. Model applications

2.4.1. Heating uniformity

After validation, the computer simulation model was used to predict the effect of different parameters on RF heating uniformity in soybeans. The heating uniformity of treated samples was evaluated by the temperature uniformity index (STUI), which is a useful tool to evaluate the heating uniformity when using a specific RF unit (Alfaifi et al., 2014):

$$\mathrm{STUI} = \frac{\int_{V_{vol}} \sqrt{(T - T_{av})^2}\, dV_{vol}}{(T_{av} - T_{initial})V_{vol}} \quad (5)$$

where T and T_{av} are local and average temperatures (°C) inside the food material over the volume (V_{vol}, m^3), $T_{initial}$ is the initial average temperature of food (°C) before RF treatments. In a RF treatment, a smaller index corresponds to better heating uniformity.

2.4.2. Simulation with varying samples moisture content

The different sample moisture content may change dielectric and thermal properties of materials, which would influence the RF heating behaviour. The dielectric properties (dielectric constant 3.5–10.4, and loss factor 0.25–7.3) of dry soybeans in different moisture content (5 ~ 10% w.b.) have been measured

Table 2 – Electrical and thermo-physical properties of dry soybeans over the tested temperature range at four moisture contents for model predictions.

Moisture content (w.b.)	Density[a] (kg m^{-3})	Thermal conductivity[b] (W m^{-1} K^{-1})	Heat capacity[c] (J kg^{-1} K^{-1})	Dielectric constant[d]	Loss factor[d]
5%	740	0.104	1737	3.5	0.25
10%	732	0.122	2030	4.81	0.9
15%	724	0.139	2323	7.12	2.63
20%	715	0.157	2616	10.4	7.3

Sources:
[a] Deshpande et al. (1993).
[b] Deshpande et al. (1996).
[c] Deshpande & Bal (1999).
[d] Guo et al. (2010).

by Guo et al. (2010) and were listed in Table 2. For density, heat capacity and thermal conductivity of dry soybeans, three well-known equations were used as a function of moisture content (w.b.) of dry soybeans by following regression formula (Deshpande & Bal, 1999; Deshpande, Bal, & Ojha, 1993, 1996):

$$\rho = 748.9(1 - 0.222m) \quad (6)$$

$$c_p = 1444(1 + 4.06m) \quad (7)$$

$$k = 8.72 \times 10^{-2}(1 + 4m) \quad (8)$$

where m is the moisture content (w.b.), ρ, c_p, and k are the bulk density (kg m^{-3}), bulk heat capacity (J kg^{-1} K^{-1}), and bulk thermal conductivity (W m^{-1} K^{-1}), respectively.

According to the above equations, a set of corresponding physical and thermal properties can be obtained based on a certain moisture content value (5 ~ 10%) (Table 2). When those parameters were inputted to the model, the corresponding STUI of samples with four different moisture contents was evaluated.

2.4.3. *Effect of top plate area and sample vertical position*

A series of simulations were run by changing top electrode areas (with the area of 830 × 400 mm^2, 400 × 300 mm^2, 350 × 250 mm^2, 300 × 220 mm^2, and 250 × 150 mm^2, respectively) progressively when dry soybean samples shaped in rectangular were placed on the ground electrode (Fig. 4). These sizes could be considered as large, medium, and small compared to the sample size. Another set of simulations was performed by varying the sample's vertical position (z = 30, 45, 60, 75, and 90 mm) between the fixed RF electrode gap (120 mm) with the top electrode size of 830 × 400 mm^2. Trends of the STUI of dry soybeans in each simulation were determined.

2.4.4. *Effect of dielectric properties and thickness of surrounding materials*

A rectangular shaped sample (300 × 220 × 60 mm^3) was placed on the ground electrode with an electrode gap of 120 mm. To study the effect of dielectric properties of surrounding materials (thickness of 150 mm) on the sample STUI, simulations

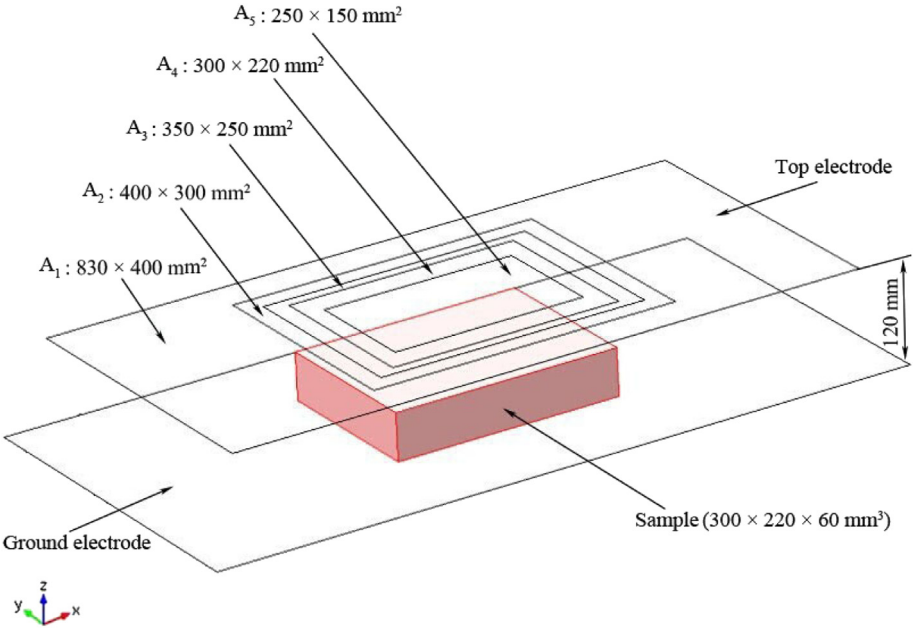

Fig. 4 – Different top electrode areas with the sample size used in the simulation.

were run with the dielectric constant ranging from 1 to 10, and loss factors of surrounding materials varying from 0.0003 to 0.3. Sample dielectric properties were fixed as $(3.6-0.26 \cdot j)$, while physical and thermal properties of surrounding materials were kept the same as those of the polypropylene container. Another set of simulations was performed in eight surrounding material thicknesses (0, 50, 100, 200, 300, 400, 500, and 600 mm) with the fixed dielectric properties $(3-0.0003 \cdot j)$ of the surrounding material.

3. Results and discussions

3.1. Simulated temperature profiles for dry soybeans

Figure 5a and b show the simulated temperature profiles of RF treated soybeans in three horizontal (20, 40, and 60 mm) and three vertical (0, 150, and 300 mm) layers with an initial temperature of 25 °C after 6 min RF heating at an electrode gap of 120 mm. In horizontal layers, the temperature values were higher in the middle and bottom layers of dry soybeans due to these layers near the bottom electrode. Because of the heat loss to the contacted container bottom, the temperatures (46.1–67.5 °C) in the bottom layer were lower than those (48.2–71.8 °C) in the middle layer. The higher temperature distribution at the middle layer could also be caused by concentrating electric field. The top layer temperatures (44.5–64.7 °C) were the lowest in three layers, which might be attributed to less concentrated electrode field distributions in the top layer and evaporative cooling in the space between the top electrode and the sample surface. In vertical layers, the sample temperature increased from the central layer to outer layers of dry soybeans, but was lower at the most outer layer, which was in contact with the container side walls. The highest temperature values were observed at the corners and edges of the top, middle and bottom layers (Fig. 5a). This heating behaviour could be attributed to the field bending and horn effects of the electromagnetic field at interfaces (Barber, 1983). Since the RF power is proportional to the square of electric field intensity, which was deflected at the sample corners and edges, net electric field increased at the corners and edges of the sample, resulting in higher temperature values at these parts (Birla, Wang, & Tang, 2008). Similar heating patterns have been observed for polyurethane foam sheets (Wang et al., 2007a), wheat flour (Tiwari et al., 2011b), and raisins (Alfaifi et al., 2014) subjected to RF treatments.

3.2. Model validation

Figure 6 shows the surface contour plot of temperature distribution obtained by experiments and computer simulation for the top, middle, and bottom layers of dry soybeans after 6 min RF heating with a fixed electrode gap of 120 mm. This comparison indicated that simulated temperature distribution patterns were in good agreement with experimental ones for all layers. Both patterns showed high temperatures at corners and edges of the top, middle, and bottom layers but low ones in the central part. The maximum temperature difference between simulation and experiment was found at corners and edges in three layers (Fig. 6). This difference could be caused by the simplification of the RF system or ignored moisture transfer from outer hot sections to inner cold sections of dry soybeans in the simulation model. The simulated temperature profile measured at the centre of second mid layer (40 mm form the container bottom) was also in good agreement with the experimental one (Fig. 7). The maximum temperature difference at the centre of second mid layer taken by an infrared camera (52 °C) and a fibre optical sensor (50 °C) was about 2 °C, which may be caused by the optical sensor tip contacted with the gauze on the second layer. A similar heating rate of 4.16 °C/min and a small RMSE of 0.012 °C were obtained between simulation and experiment over the heating period (Fig. 7). Table 3 compared the simulated and experimental average and standard deviation temperatures of soybean samples in all three horizontal layers after 6 min RF heating. The experimental average temperatures at top and bottom layers were slightly lower than

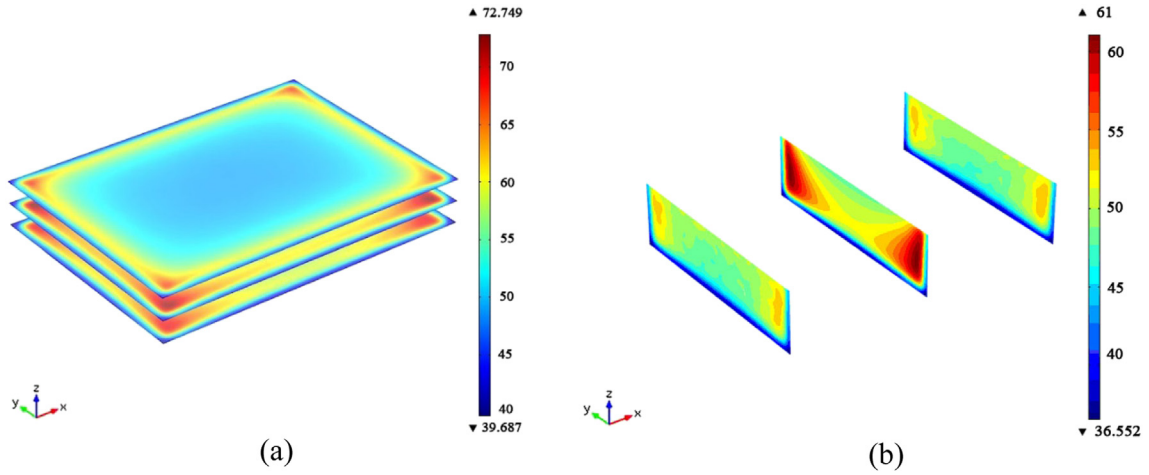

Fig. 5 – Simulated temperature (°C) profiles of dry soybeans (300 × 220 × 60 mm³) at three horizontal layers (20, 40, and 60 mm) (a) and three vertical layers (0, 150, and 300 mm) (b), after 6 min RF heating with an electrode gap of 120 mm and initial temperature of 25 °C.

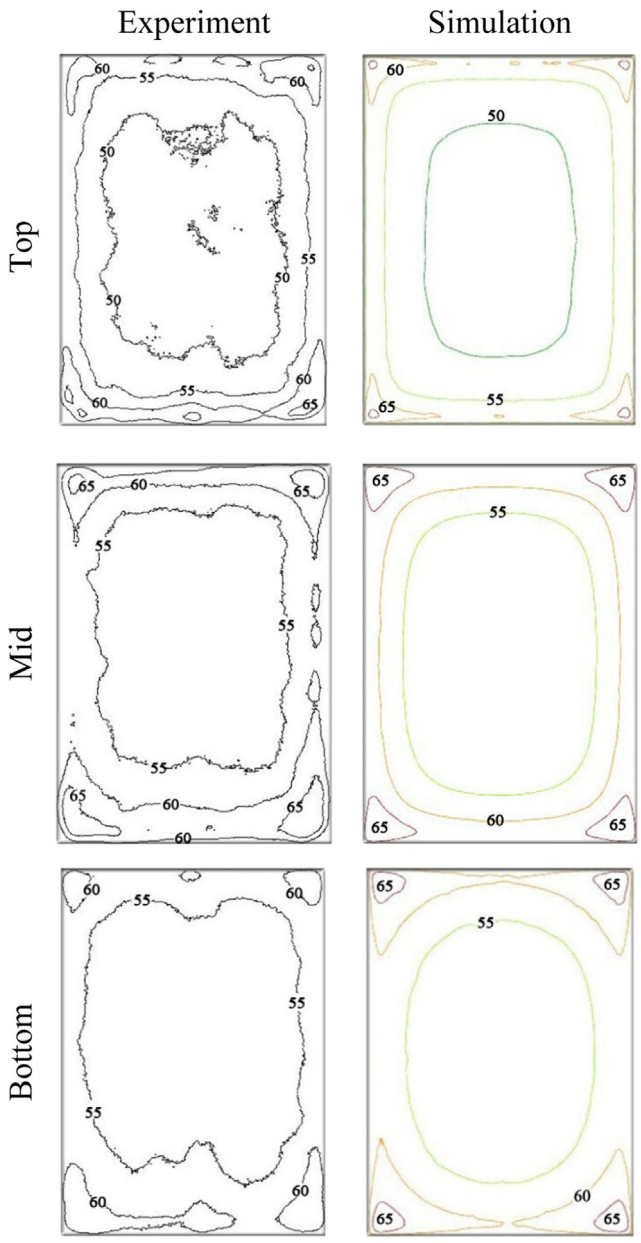

Fig. 6 – Experimental and simulated temperature distributions (°C) of dry soybeans in top, middle, and bottom layers (20, 40, and 60 mm from the bottom of sample) placed in a polypropylene container (300 × 220 × 60 mm³) on the bottom electrode, after 6 min RF heating with an initial temperature of 25 °C and a fixed electrode gap of 120 mm.

simulated ones, which were probably caused by heat loss to the environment due to later measurement after RF heating. However, the simulated standard deviation was relatively higher than that determined by experiments. This was probably caused by more data points for corners with fined meshes than those at the centre in simulation, while these are equally distributed in the experiment. On the other hand, the extreme sample temperatures were reduced due to later mapping after RF heating in the experiment.

3.3. *Effect of sample moisture content on STUI*

Figure 8 illustrates the effect of sample moisture content on STUI of dry soybeans. Modifying samples moisture content caused the change of dielectric, thermal properties, and density of dry soybeans. Simulated results demonstrated that increasing sample moisture content caused gradual increase of STUI, which was mainly influenced by the relationship between electrical and thermo-physical properties of dry soybeans and moisture contents (Table 2). Values of STUI were higher when sample moisture content increased, indicating that the smaller moisture content resulted in better temperature uniformities in samples. The higher moisture contents along with the larger dielectric and thermal properties, resulting in higher STUI values, that is, poor RF heating uniformity. So RF is more suitable for dry products treatment based on the achievable heating uniformity.

3.4. *Effect of top plate areas on STUI*

Figure 9 shows the effect of top plate area on the sample STUI. The results showed that the top electrode areas (lengths and widths) greatly affected the sample STUI. Decreasing top electrode areas with five different values caused initial reduction and then the increase of STUI. STUI was the lowest when the top electrode areas were changed between 400 × 300 mm² and 300 × 220 mm², 1 ~ 1.81 times of the sample size (300 × 220 mm²). When the top electrode area was changed into 350 × 250 mm² (1.32 times of the sample size), the STUI was 0.083, which was lower than that (0.098) for areas of 300 × 220 mm² (the sample surface area). With a decrease of the top plate area, the electric field distribution within the sample also changed. When the top plate area was comparatively larger than that of the sample size, most of the electric field entered obliquely into the sample, which could be mainly deflected by sample edges and corners. The concentrated electric field would increase the temperature non-uniformity in the sample. When the top plate area was changed to 1.32 times of the sample size, the electric field started entering normally into the sample, and thus the hot spot in corners and edges of sample would be largely reduced. With a further decrease of the top plate area, the electric field would not be able to enter into the sample completely and the sample could not be fully heated, causing the enhanced temperature non-uniformity again. So the heating uniformity was improved by a small top electrode (350 × 250 mm²) as compared to a large and original top electrode area of 830 × 400 mm². The maximum temperature of middle layers was reduced from 71 °C to 57 °C, while minimum temperature was maintained at the same 50 °C (Fig. 10). Similar heating behaviour has been observed for wheat flour, in which RF power uniformity was the highest when sample lengths and widths lied between 35 ~ 50% of the top electrode size during RF treatment (Tiwari et al., 2011b).

3.5. *Effect of sample vertical positions on STUI*

The effect of sample vertical positions on STUI was assessed using the simulation model as shown in Fig. 11.

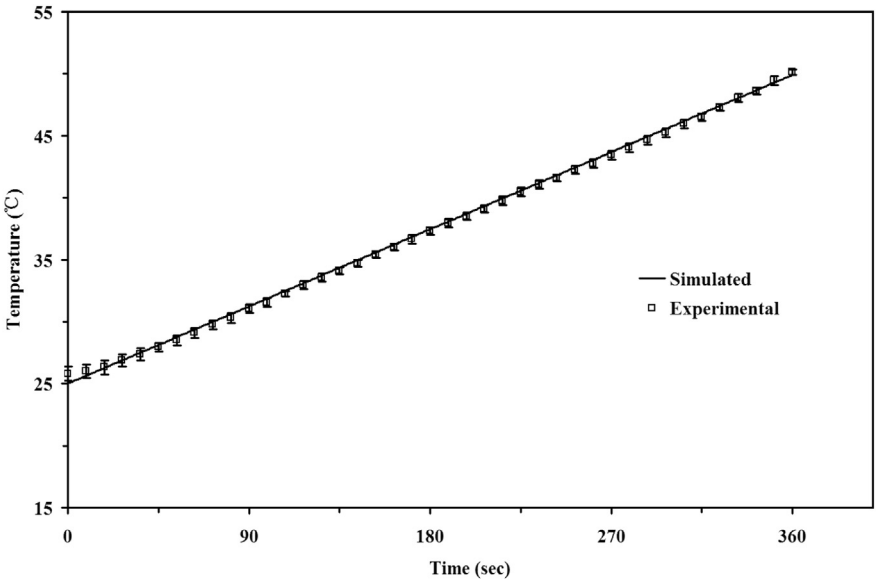

Fig. 7 – Experimental and simulated temperature–time histories of dry soybeans at the centre of second mid layer (40 mm) from the bottom of sample (300 × 220 × 60 mm^3), placed in a polypropylene container on the grounded electrode during 6 min RF heating with an electrode gap of 120 mm.

The STUI decreased first and then increased when a sample vertical position (along z axis) was changed from the bottom to the top electrode. When samples were placed on the bottom electrode (z = 30 mm), STUI was higher than that in the centre position (z = 60 mm). When samples were placed in touch with the top electrode (z = 90 mm), STUI was the highest compared with other positions. This phenomenon can be caused by the increased electric field concentration at contact surfaces. As shown in Fig. 11, STUI was the lowest when samples were placed in the middle (z = 60 mm) of RF electrodes as electric field deflected by top and bottom edges increased net electric field concentration at the central part of samples (Marra et al., 2007). The similar results have been also obtained by Birla, Wang, and Tang (2008) and Tiwari et al. (2011b) that when the small size sample is placed in the middle of RF electrodes, the power uniformity would be clearly improved. This suggests that the good RF heating uniformity should be obtained in samples when positions were located in the middle of the electrode gap.

Table 3 – Comparison between simulated and experimental average (Ave) and standard deviation (SD) temperatures (°C) of dry soybeans at three horizontal layers after 6 min RF heating at a fixed electrode gap of 120 mm and initial temperature of 25 °C.

Layer	Simulated		Experimental	
	Ave	SD	Ave	SD
Top	52.82	4.44	52.79	3.86
Middle	55.20	6.49	55.85	4.38
Bottom	54.23	5.66	53.65	4.63

3.6. *Effect of dielectric materials around samples on STUI*

Figure 12 shows the effect of the surrounding material dielectric constant with three different loss factors on STUI with the given sample dielectric properties of 3.6–0.26·*j*. STUI decreased with decreasing loss factor due to reduced RF power absorption, especially at the dielectric constant of around 3. STUI decreased first, and then increased with increasing surrounding material dielectric constant for each given loss factor. STUI was the lowest when the surrounding material dielectric constant was between 2.5 and 3.5, suggesting that the temperature uniformity could be achieved when the surrounding material dielectric constant was approaching to the sample one. It is well known that if the loss factor is far smaller than the dielectric constant, the dielectric constant is dominating the electric field distribution (Metaxas, 1996). Therefore, if a proper material with a low loss factor and a similar dielectric constant to that of dry soybeans can be added to surround the soybean sample, instead of air, a more uniform electric field can be produced in the sample, which resulted in a better heating uniformity. On the middle layers, the difference between maximum and minimum temperatures was found to be reduced from 24 to 15 °C using similar dielectric constant material, which implies a better heating uniformity. The similar computer simulation results on RF power uniformity index have been reported in wheat flour (Tiwari et al. 2011b).

Results in Fig. 13 show the thickness effect of the surrounding material with a similar dielectric constant (3) to that of dry soybeans on the sample STUI. STUI showed a sharp decrease first and then a constant as a function of material thickness. When the thickness of the surrounding material lied between 100 and 200 mm for the side walls of the

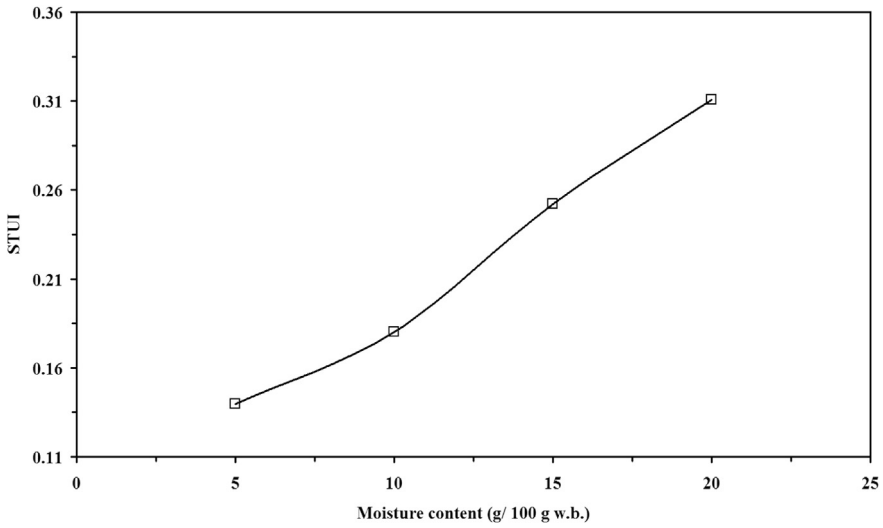

Fig. 8 – Simulated temperature uniformity index (STUI) of rectangular shaped dry soybeans with varying moisture content. Sample size (300 × 220 mm^2) and heights were set as 60 mm. Container was placed on the bottom electrode with a fixed gap of 120 mm.

rectangular plastic container, STUI was the lowest compared to other thicknesses. While the surrounding material thickness is in a reasonable range, the better temperature uniformity can be achieved since the electric field started entering normally into the centre of the whole treated material (Tiwari et al., 2011b). Generally, strong electromagnetic fields are concentrated in corners and edges of a rectangular shaped sample, causing higher temperatures in these locations (Datta & Zhang, 2001), especially for relatively small samples as compared to the top electrode area. If the thickness of the surrounding material (with a similar dielectric constant to that of sample) increased, the non-uniform heating at edges and corners of the sample would be improved as the entire heated material geometry size increased due to reduced electromagnetic fields at sample edges or corners and increased energy absorption of the surrounding materials. When the surrounding material thickness >200 mm, the width of the whole treated material surpass the top electrode's width, resulting in the slightly increased STUI since no electric field entering into those outside regions. When the material thickness is more than 200 mm, on the other hand, the overall average temperature of the whole food sample would be reduced gradually. According to Eq. (5), the STUI may not be further reduced since the slightly improved temperature difference between sample edge and centre is balanced by the reduced average sample temperature.

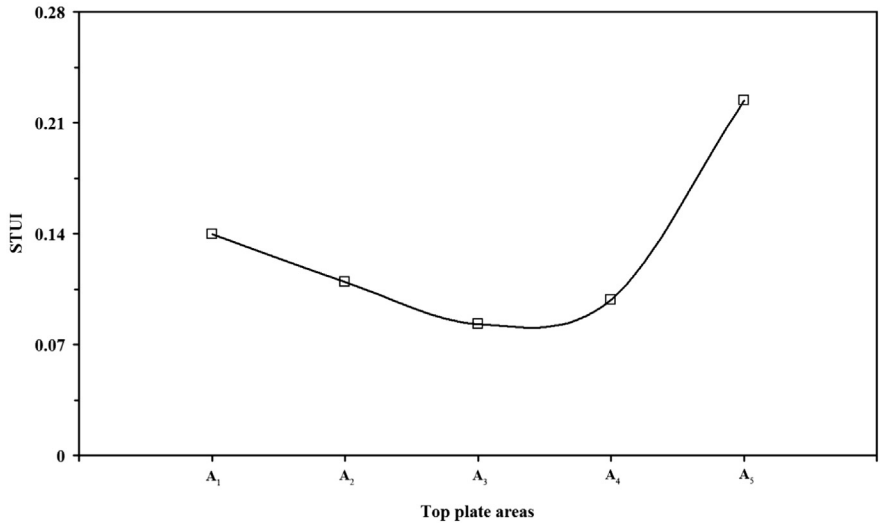

Fig. 9 – Simulated temperature uniformity index (STUI) of dry soybeans in a rectangular container (300 × 220 × 60 mm^3) with varying top plate areas (A_1: 830 × 400 mm^2, A_2: 400 × 300 mm^2, A_3: 350 × 250 mm^2, A_4: 300 × 220 mm^2, and A_5: 250 × 150 mm^2). Container was placed on the bottom electrode with a fixed gap of 120 mm.

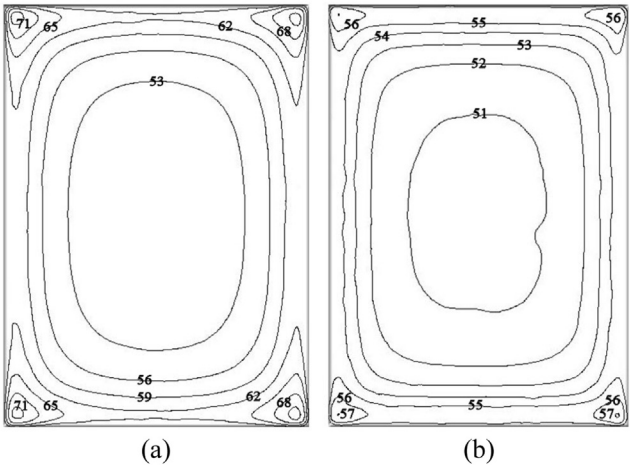

Fig. 10 – Simulated temperature distributions of dry soybeans in a rectangular container (300 × 220 × 60 mm^3 with top plate areas of (a) 830 × 400 mm^2, and (b) 350 × 250 mm^2. Container was placed on the bottom electrode with a fixed gap of 120 mm.

3.7. *General applications of simulation results to improve RF heating uniformity*

This simulation is performed by targeting temperatures of 55–60 °C required by developing postharvest RF disinfestation treatments (Jiao et al., 2012; Wang et al., 2007b; Zhao et al., 2007). Although absolute values of STUI could be different, the findings, such as a surrounding material with similar dielectric constant to that of sample and appropriate thickness, placing the sample in the middle of electrodes, and using similar top electrode size to that of the sample, should be practical to improve RF heating uniformity in other dry products, such as lentils, almonds, walnuts etc., and other applications, such as drying, pasteurization, and enzyme inactivation (Gao, Tang, Villa-Rojas, Wang, & Wang, 2011; Marra et al., 2007; Marshall & Metaxas, 1998). The model results have been validated by experimental temperature distributions over three layers of soybeans in a container. With the limited temperature data, efficacy tests with placing randomly live insects in the container could be conducted together with product quality evaluation to further confirm the RF heating uniformity in large containers. This uniformity study would be served as a first step for developing an effective RF treatment protocol.

4. Conclusions

A computer simulation model using a finite element based commercial software COMSOL was used to evaluate the RF heating uniformity. Experiments were conducted with dry soybeans in a rectangular plastic container to validate the simulation model. The experimental results were in good agreement with the simulation ones, and both showed higher temperature values in the middle and bottom layers compared with those of the top layers. Corners and edges were heated more than centre areas in all layers. The validated computer simulation model was applied to simulate effects of various factors, such as top plate area, sample moisture content, sample vertical position, and dielectric materials around samples on the simulated results. Simulated results showed that the smaller top plate area (similar to the sample size), placing the sample in the middle of two electrodes, and surrounding container with a similar dielectric constant sheets to sample one provided better RF heating uniformity since the maximum and minimum temperature difference in middle layers was reduced from 24 to 15 °C. The developed simulation model is an effective tool to understand and analyse the complexity of RF heating behaviour and to

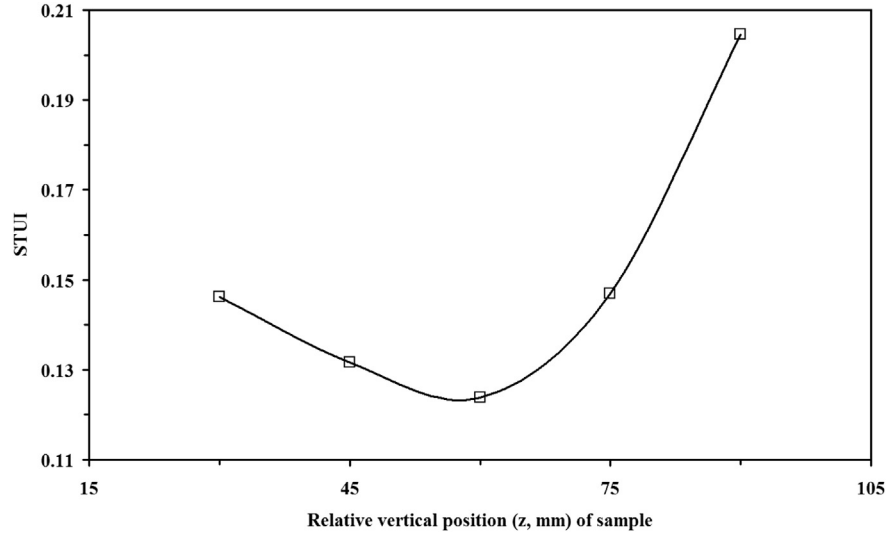

Fig. 11 – Simulated temperature uniformity index (STUI) of rectangular shaped dry soybean samples with thicknesses of 60 mm, kept at five different vertical positions (along z axis) of top electrode size (830 × 400 mm^2) under a fixed electrode gap of 120 mm.

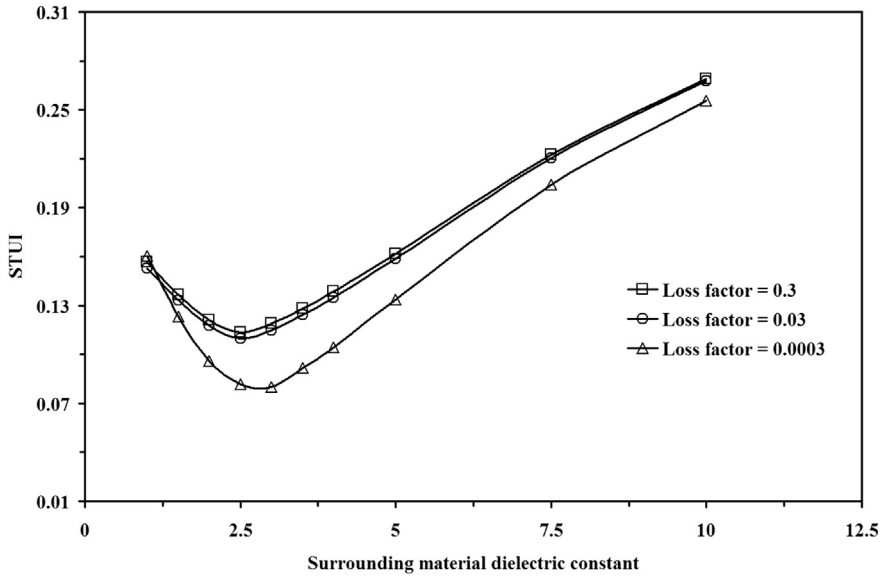

Fig. 12 – Simulated temperature uniformity index (STUI) in a sample (300 × 220 × 60 mm^3) with varying surrounding material (thickness of 150 mm) dielectric constants at three loss factors. Sample dielectric properties were fixed as (3.6–0.26·*j*) with top electrode size (830 × 400 mm^2) and kept on the bottom electrode with a fixed gap of 120 mm.

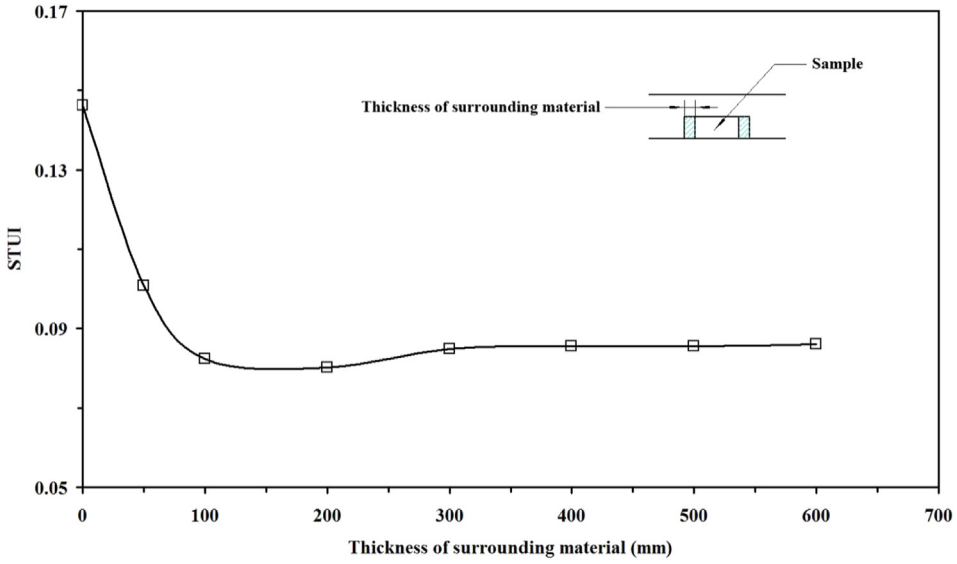

Fig. 13 – Simulated temperature uniformity index (STUI) of rectangular shaped dry soybeans with varying surrounding material thickness. Sample size (300 × 220 mm^2) and heights were set as 60 mm with top electrode size (830 × 400 mm^2). Container was placed on the bottom electrodes with a fixed gap of 120 mm.

improve temperature distributions in other dry products and applications.

Acknowledgements

This research was conducted in the College of Mechanical and Electronic Engineering, Northwest A&F University, and supported by research grants from Ph.D. Programs Foundation of Ministry of Education of China (20120204110022) and General Program of National Natural Science Foundation of China (31371853). The authors thank Qian Hao, Bo Ling, Rui Li, and Lixia Hou for their helps in conducting experiments.

REFERENCES

Alfaifi, B., Tang, J., Jiao, Y., Wang, S., Rasco, B., Jiao, S., et al. (2014). Radio frequency disinfestation treatments for dry fruit: model

development and validation. *Journal of Food Engineering, 120*, 268–276.
Barber, H. (1983). *Electroheat* (1st ed.). London, UK: Granada Publishing Limited.
Birla, S., Wang, S., & Tang, J. (2008). Computer simulation of radio frequency heating of model fruit immersed in water. *Journal of Food Engineering, 84*(2), 270–280.
Birla, S., Wang, S., Tang, J., & Tiwari, G. (2008). Characterization of radio frequency heating of fresh fruits influenced by dielectric properties. *Journal of Food Engineering, 89*(4), 390–398.
Chan, T., Tang, J., & Younce, F. (2004). 3-Dimensional numerical modeling of an industrial radio frequency heating system using finite elements. *Journal of Microwave Power and Electromagnetic Energy, 39*(2), 87–105.
Choi, C., & Konrad, A. (1991). Finite element modeling of the RF heating process. *IEEE Transactions on Magnetics, 27*(5), 4227–4230.
COMSOL material library. (2012). *COMSOL Multiphysics, V4.3a*. Burlington, MA, USA.
Datta, K., & Zhang, H. (2001). Electromagnetics of microwave heating: Magnitude and uniformity of energy absorption in an oven. In *Handbook of microwave technology for food applications*. New York: Marcel Dekker, Inc.
Deshpande, S., & Bal, S. (1999). Specific heat of soybean. *Journal of Food Process Engineering, 22*(6), 469–477.
Deshpande, S., Bal, S., & Ojha, T. (1993). Physical properties of soybean. *Journal of Agricultural Engineering Research, 56*(2), 89–98.
Deshpande, S., Bal, S., & Ojha, T. (1996). Bulk thermal conductivity and diffusivity of soybean. *Journal of Food Processing and Preservation, 20*(3), 177–189.
Fu, Y. C. (2004). Fundamentals and industrial applications of microwave and radio frequency in food processing. In *Food processing: Principles and applications* (pp. 79–100). Iowa, USA: Blackwell.
Gao, M., Tang, J., Villa-Rojas, R., Wang, Y., & Wang, S. (2011). Pasteurization process development for controlling *Salmonella* in in-shell almonds using radio frequency energy. *Journal of Food Engineering, 104*(2), 299–306.
Guo, W., Wang, S., Tiwari, G., Johnson, J. A., & Tang, J. (2010). Temperature and moisture dependent dielectric properties of legume flour associated with dielectric heating. *LWT–Food Science and Technology, 43*(2), 193–201.
Halverson, S. L., Burkholder, W. E., Bigelow, T. S., Nordheim, E. V., & Misenheimer, M. E. (1996). High-power microwave radiation as an alternative insect control method for stored products. *Journal of Economic Entomology, 89*(6), 1638–1648.
von Hippel, A. R. (1995). *Dielectric materials and applications*. Boston, USA: Arctech House.
Jiao, S., Johnson, J., Tang, J., & Wang, S. (2012). Industrial-scale radio frequency treatments for insect control in lentils. *Journal of Stored Products Research, 48*, 143–148.
Jiao, S., Tang, J., Johnson, J. A., Tiwari, G., & Wang, S. (2011). Determining radio frequency heating uniformity in mixed beans for disinfestations. *Transactions of the ASABE, 54*(5), 1847–1855.
Lagunas-Solar, M., Pan, Z., Zeng, N., Truong, T., Khir, R., Amaratunga, K., et al. (2007). Application of radiofrequency power for non-chemical disinfestation of rough rice with full retention of quality attributes. *Applied Engineering in Agriculture, 23*(5), 647.
Marra, F., Lyng, J., Romano, V., & McKenna, B. (2007). Radio-frequency heating of foodstuff: solution and validation of a mathematical model. *Journal of Food Engineering, 79*(3), 998–1006.
Marshall, M. G., & Metaxas, A. C. (1998). Modeling of the radio frequency electric field strength developed during the RF assisted heat pump drying of particulates. *Journal of Microwave Power and Electromagnetic Energy, 33*(3), 167–177.
Metaxas, A. C. (1996). *Foundations of electroheat-a unified approach*. New York: John Wiley & Sons.
Mitcham, E., Veltman, R., Feng, X., De Castro, E., Johnson, J., Simpson, T., et al. (2004). Application of radio frequency treatments to control insects in in-shell walnuts. *Postharvest Biology and Technology, 33*(1), 93–100.
Nelson, S. O. (1973). Insect-control studies with microwaves and other radiofrequency energy. *Bulletin of the ESA, 19*(3), 157–163.
Nelson, S. (1996). Review and assessment of radio-frequency and microwave energy for stored-grain insect control. *Transactions of the ASAE, 39*(4), 1475–1484.
Neophytou, R. I., & Metaxas, A. C. (1996). Computer simulation of a radio frequency industrial system. *Journal of Microwave Power and Electromagnetic Energy, 31*(4), 251–259.
Neophytou, R., & Metaxas, A. (1998). Combined 3D FE and circuit modeling of radio frequency heating systems. *Journal of Microwave Power and Electromagnetic Energy, 33*(4), 243–262.
Neophytou, R., & Metaxas, A. (1999). Combined tank and applicator design of radio frequency heating systems. *IEEE Proceedings-Microwaves Antennas and Propagation, 146*(5), 311–318.
Romano, V., & Marra, F. (2008). A numerical analysis of radio frequency heating of regular shaped foodstuff. *Journal of Food Engineering, 84*(3), 449–457.
Tang, J., Ikediala, J. N., Wang, S., Hansen, J., & Cavalieri, R. (2000). High-temperature-short-time thermal quarantine methods. *Postharvest Biology and Technology, 21*, 129–145.
Tiwari, G., Wang, S., Tang, J., & Birla, S. (2011a). Computer simulation model development and validation for radio frequency (RF) heating of dry food materials. *Journal of Food Engineering, 105*(1), 48–55.
Tiwari, G., Wang, S., Tang, J., & Birla, S. (2011b). Analysis of radio frequency (RF) power distribution in dry food materials. *Journal of Food Engineering, 104*(4), 548–556.
[USADPLC] USA Dry Pea & Lentil Council. (2007). *Policy position about trade barrier and restrictions*. Moscow, ID.
Wang, S., Ikediala, J. N., Tang, J., Hansen, J. D., Mitcham, E., Mao, R., et al. (2001). Radio frequency treatments to control codling moth in in-shell walnuts. *Postharvest Biology and Technology, 22*, 29–38.
Wang, S., Monzon, M., Johnson, J., Mitcham, E., & Tang, J. (2007a). Industrial-scale radio frequency treatments for insect control in walnuts: I: heating uniformity and energy efficiency. *Postharvest Biology and Technology, 45*(2), 240–246.
Wang, S., Monzon, M., Johnson, J., Mitcham, E., & Tang, J. (2007b). Industrial-scale radio frequency treatments for insect control in walnuts: II: Insect mortality and product quality. *Postharvest Biology and Technology, 45*(2), 247–253.
Wang, J., Olsen, R. G., Tang, J., & Tang, Z. (2008). Influence of mashed potato dielectric properties and circulating water electric conductivity on radio frequency heating at 27 MHz. *Journal of Microwave Power and Electromagnetic Energy, 42*(2), 31–46.
Wang, S., Tang, J., Sun, T., Mitcham, E., Koral, T., & Birla, S. (2006). Considerations in design of commercial radio frequency treatments for postharvest pest control in in-shell walnuts. *Journal of Food Engineering, 77*(2), 304–312.
Wang, S., Tiwari, G., Jiao, S., Johnson, J., & Tang, J. (2010). Developing postharvest disinfestation treatments for legumes using radio frequency energy. *Biosystems Engineering, 105*(3), 341–349.
Wang, S., Yue, J., Tang, J., & Chen, B. (2005). Mathematical modelling of heating uniformity for in-shell walnuts subjected to radio frequency treatments with intermittent stirrings. *Postharvest Biology and Technology, 35*(1), 97–107.

Wilcox, J. R. (2004). World distribution and trade of soybean. In *Soybeans: Improvement, production, and uses* (pp. 1–14). USA: American Society of Agronomy.
Yang, J., Zhao, Y., & Wells, J. H. (2003). Computer simulation of capacitive radio frequency (RF) dielectric heating on vegetable sprout seeds. *Journal of Food Process Engineering, 26*(3), 239–263.
Zhao, S., Qiu, C., Xiong, S., & Cheng, X. (2007). A thermal lethal model of rice weevils subjected to microwave irradiation. *Journal of Stored Products Research, 43*(4), 430–434.